

FULL PAPER

# Design, synthesis, biological evaluations, molecular docking, and *in vivo* studies of novel phthalimide analogs

Magdy A. H. Zahran<sup>1</sup> | Bishoy El-Aarag<sup>2</sup> | Ahmed B. M. Mehany<sup>3</sup> |  
Amany Belal<sup>4</sup>  | Ali S. Younes<sup>1</sup>

<sup>1</sup> Faculty of Science, Department of Chemistry, Menoufia University, Shebin El-Koom, Egypt

<sup>2</sup> Biochemistry Division, Faculty of Science, Department of Chemistry, Menoufia University, Shebin El-Koom, Egypt

<sup>3</sup> Faculty of Science, Department of Zoology, Al-Azhar University, Cairo, Egypt

<sup>4</sup> Faculty of Pharmacy, Department of Medicinal Chemistry, Beni-Suef University, Beni-Suef, Egypt

## Correspondence

Dr. Amany Belal, Faculty of Pharmacy, Department of Medicinal Chemistry, Beni-Suef University, Beni-Suef 62514, Egypt.  
Email: abilalmoh1@yahoo.com

## Abstract

A series of novel phthalimide analogs containing an indole or brominated indole moiety were synthesized and their antimicrobial activity was evaluated. Compound **8** showed a broad spectrum activity, revealing 53–67% of erythromycin activity on the tested bacteria and 60–70% of miconazole activity on the tested fungi. Anticancer activity was evaluated on the cell lines HepG2, MCF-7, A549, H1299, and Caco2. The results revealed that the new phthalimide analog **8** has broad-spectrum anticancer activity toward all the tested cancer cell lines, followed by compound **11**, which showed good activity toward all the tested cell lines except for MCF-7. The ability of the promising analogs **5**, **8**, and **11** to bind to topoisomerase II DNA gyrase was investigated. Caspase-3 activation and Bcl-2 assay of the best active derivatives **8**, **11** in addition to compound **5** were evaluated. The antifibrotic activity was studied in an *in vivo* model and the histopathological studies revealed that treatment with the new compound **8** improved the fibrotic liver tissues to normality.

## KEYWORDS

caspase-3, gyrase binding mode, indole derivatives, liver fibrosis, phthalimide analogs, thalidomide

## 1 | INTRODUCTION

Cancer is a disease characterized by the uncontrolled growth and spread of abnormal cells. It is caused by external factors, such as smoking, infectious organisms, an unhealthy diet and internal factors such as inherited genetic mutations, hormones, and immune conditions. Treatments include surgery, chemotherapy, radiation, hormone, and immune therapy.<sup>[1]</sup> It was estimated that the number of deaths attributed to cancer would rise to an annual 19.3 million by 2025.<sup>[2]</sup> Therefore, the research for new cancer-treating agents is an important area in both organic and medicinal chemistry. Recently, many heterocyclic compounds possessing biologically active properties have been synthesized and evaluated as anticancer drug candidates. Among these biologically active heterocycles, phthalimide is an important pharmacophore and has a privileged structure in drug discovery. It has been reported

that the phthalimide moiety is a very important biologically active pharmacophore.<sup>[3–6]</sup> Antimicrobial properties of phthalimide derivatives were reported.<sup>[7–12]</sup> Compounds **IV** and **V** (Figure 1) exhibited high antimicrobial activities against the tested microorganisms.<sup>[8]</sup> Isoindole-1,3-dione is a building unit in antitumor,<sup>[13,14]</sup> antiangiogenic<sup>[15]</sup> as well as immunomodulatory drug candidates.<sup>[16,17]</sup> Thalidomide (Figure 1) is a drug known to have antiangiogenic, immunomodulatory and significant antitumor activities, its analogs showed significant potency against several diseases such as prostate cancer, HIV-related ulcers, multiple myeloma, and Kaposi's sarcoma; this drug consists of two heterocyclic moieties: the phthalimide, and the piperidine-2,6-dione moiety.<sup>[18–20]</sup> Indole-based compounds **I–III** (Figure 1) are well known in the medicinal chemistry research as antimicrobial, anticancer,<sup>[21–24]</sup> antifungal, and antibacterial<sup>[25]</sup> active agents. Figure 1 illustrates the structure of indole-based derivatives and the strategy for designing our target compounds.

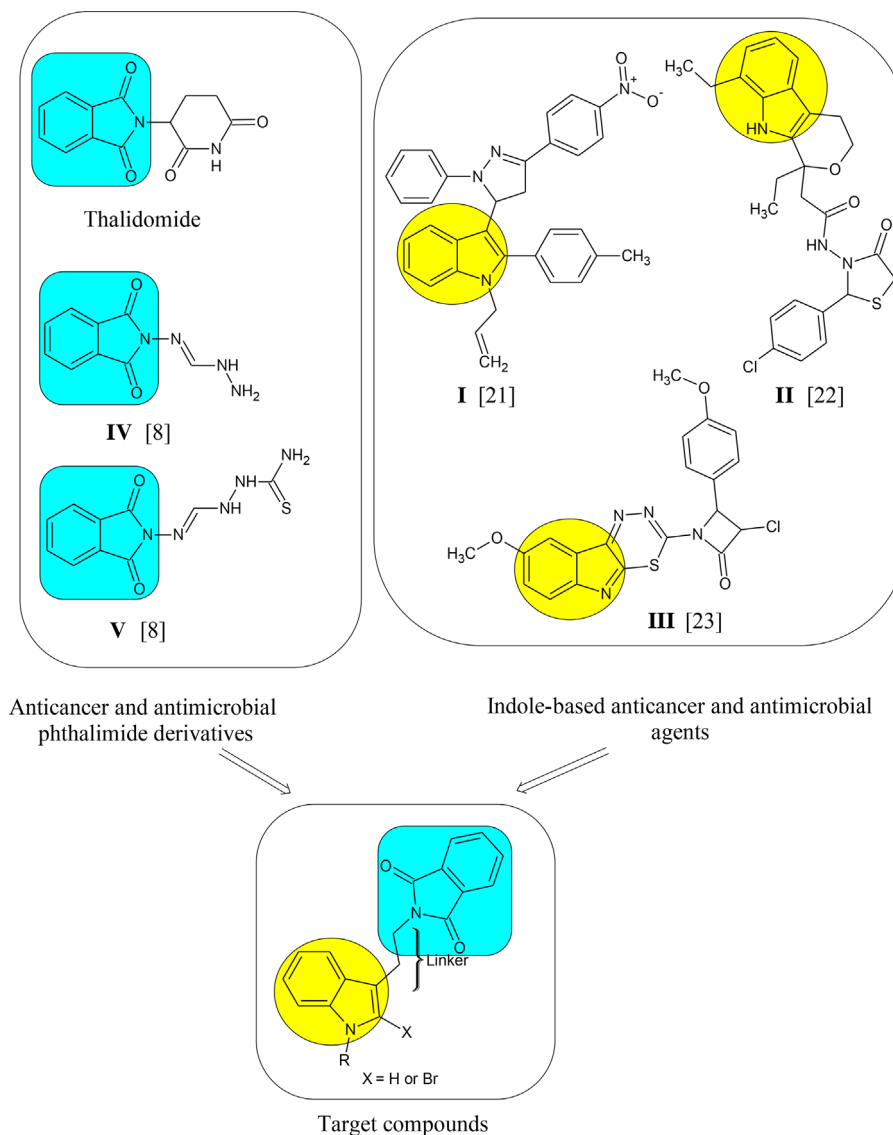


**FIGURE 1** Molecular design of the novel phthalimide–indole hybrids

Tryptamine (indole-3-ethylamine) and its derivatives have high pharmaceutical significance because of their naturally occurring as well as their utility in several drugs.<sup>[26]</sup> Tryptamine derivatives are used in the treatment of migraine, obesity and behave as antitumor active analogs.<sup>[27–30]</sup>

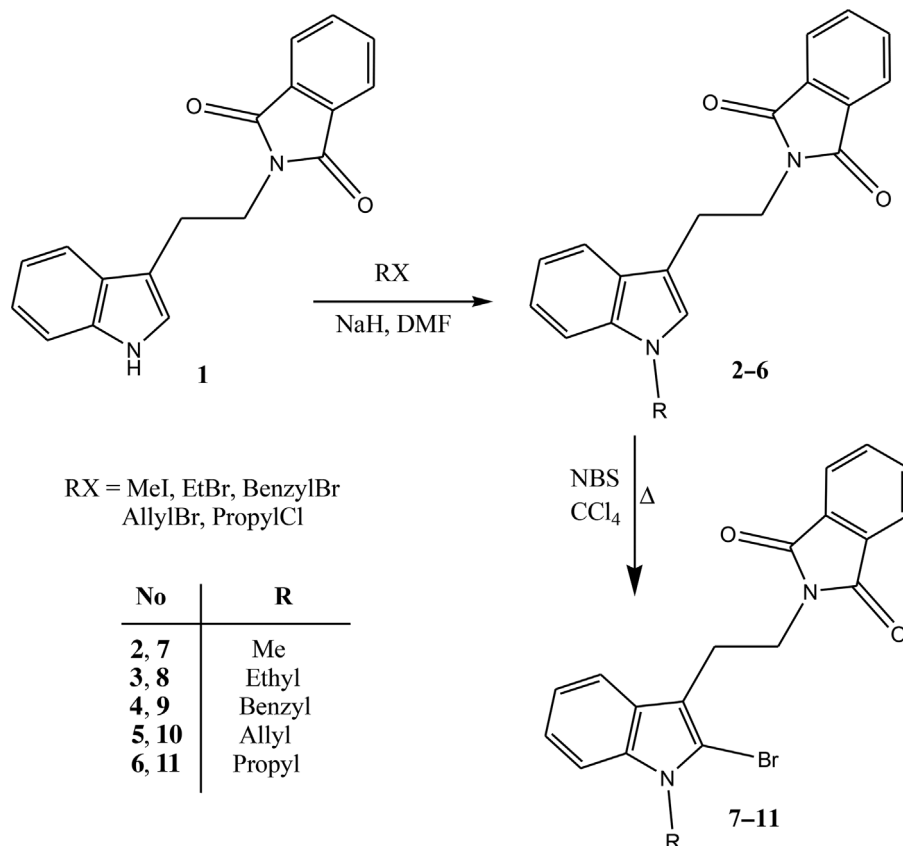
Based on our previous studies which involved the synthesis and evaluation of novel thalidomide analogs as anticancer and antiangiogenic agents<sup>[31–36]</sup> and the diversity of biological activities of indole derivatives, the current study aimed to synthesize and evaluate novel phthalimide–indole hybrids as antimicrobial, antitumor, and anti-hepatic fibrosis agents.

## 2 | RESULTS AND DISCUSSION

### 2.1 | Chemistry

The current study includes the synthesis of analogs 2–11 by alkylation of indole at N<sub>1</sub> using different alkylating agents and followed by

bromination at position 2 of indole to afford compounds 7–11 (Scheme 1). The indolyisindoldione 1, the alkylated analogs 2 and 4 were prepared according to the previously reported procedures.<sup>[37,38]</sup> The analog 3 was obtained by alkylation of 1 by ethyl bromide in the presence of NaH. The melting point (m.p.) of derivative 3 closely matches the reported data.<sup>[39,40]</sup> The <sup>1</sup>H NMR spectrum of derivative 5 showed signals at 3.85 ppm for N-CH<sub>2</sub>, multiplet signal at 5.90 ppm for olefinic CH, and doublet signal at 5.02 ppm for terminal CH<sub>2</sub>. The <sup>1</sup>H NMR analysis for isoindole derivative 6 revealed triplet signal at 3.84 ppm for N-CH<sub>2</sub>, multiplet signal at 1.67 ppm for CH<sub>2</sub>, and triplet signal at 0.72 ppm for terminal CH<sub>3</sub>. Characteristic singlet peak of 2-H of indole ring appears in the <sup>1</sup>H NMR spectra of derivatives 5 and 6 at 7.14 and 7.16 ppm, respectively. Derivatives 2–6 were brominated using NBS in CCl<sub>4</sub> under reflux to afford brominated isoindole derivatives 7–11. The <sup>1</sup>H NMR spectra of the derivatives 7–11 have no singlet peak of 2-H of indole ring in the aromatic area indicating that the substitution of that proton was successfully done. The <sup>13</sup>C NMR,



**SCHEME 1** Synthesis of N-alkylated and 2-brominated indolyl isoindole analogs 2-11

mass and elemental analysis were also used to elucidate the structures of all new isoindole derivatives.

## 2.2 | Biological activities

### 2.2.1 | Antimicrobial activity

The antimicrobial activity of the synthesized analogs against gram positive bacteria (*Bacillus subtilis* ATCC 6633, *Staphylococcus aureus* ATCC 35556), gram negative bacteria (*Escherichia coli* ATCC 23282 and *Pseudomonas aeruginosa* ATCC 10145), fungi (*Candida albicans* IMRU 3669), and filamentous fungus (*Aspergillus niger* ATCC 16404) was evaluated. Concerning the gram positive bacteria, results in Table 1 revealed that compounds 5 and 6 have a good activity on *B. subtilis*, their activity was 68 and 64% of erythromycin activity, respectively. Analogs 3, 5, 6, 10, and 11 showed moderate activity against *S. aureus*, their activity was 53% of erythromycin activity, however, analogs 4 and 8 showed better activity against the same tested microorganism with 60% of erythromycin activity. Concerning the gram negative bacteria, analogs 4 and 5 showed good activities on *E. coli*, their activity was 63% of erythromycin activity. Analog 8 showed two thirds the activity of erythromycin on *E. coli* but analog 11 showed 59% of erythromycin activity. Analogs 5 and 8 are the best active on *P. aeruginosa* followed by analog 6 with a percent of inhibition equal 65, 65, and 62% of erythromycin activity, respectively. Screening of synthesized analogs against fungi (*C. albicans* and *Asp. niger*)

revealed that analogs 4, 8, 10, and 11 showed good activity against *C. albicans*, their activities were 61, 61, 65, and 69% of miconazole activity, respectively, followed by compound 3 that showed 59% of miconazole activity. Analogs 3, 4, 8-11 showed to be active against *Asp. niger*, their activities ranged from 60 to 70% of miconazole activity.

### 2.2.2 | Antiproliferative activity

The synthesized analogs were tested against MCF-7, Caco2, HepG2, H1299, and A549 cells using SRB assay and thalidomide as a reference drug. IC<sub>50</sub> values are reported in Table 2. The tested analogs showed activity toward HepG2 cell line, especially analogs 5, 7-11 with cytotoxicity ranging from 53.3 to 69.6 μM, compared to thalidomide (193.6 μM). All analogs showed good activity on Caco2 cell line, with IC<sub>50</sub> values less than that of thalidomide except compounds 2 and 6. Concerning H1299 cell line, analogs 6, 8, and 11 showed activity more than that of thalidomide, their IC<sub>50</sub> values are less than 50 μM. Analogs 8, 10, and 11 showed potent effect on A549 compared to the reference drug. Analog 8 showed anticancer activity toward MCF-7 cell line comparable with that of thalidomide.

The undesirable damage to normal cells triggered by the high toxicity of anticancer drugs is one of the chief complications of cancer chemotherapy. The most active compounds against the studied cancer cell lines that caused the highest apoptotic effect were selected to be tested for cytotoxicity against normal liver cell line (THLE-2) and their IC<sub>50</sub> values were determined. Results demonstrated that the selected

**TABLE 1** Antimicrobial activity of phthalimide analogs on different microorganisms

Analog	Inhibition zone (mm) of microorganism					
	Bacteria				Fungi	
	<i>Bacillus subtilis</i>	<i>Staph. aureus</i>	<i>Escherichia coli</i>	<i>Pseud. aeruginosa</i>	<i>Candida albicans</i>	<i>Aspergillus niger</i>
2	15	12	14	15	14	12
3	15	15	14	14	15	16
4	16	17	17	16	16	17
5	19	15	17	19	12	12
6	18	15	15	18	13	13
7	12	13	12	15	12	12
8	15	17	18	19	16	19
9	14	13	14	16	14	16
10	16	15	14	15	17	18
11	15	15	16	17	18	19
Erythromycin	28	28	27	29	-	-
Miconazole	-	-	-	-	26	27

The experiments were done in duplicates.

compounds **5**, **8**, and **11** exhibited  $IC_{50}$  ( $\mu M$ ) values of 951.27, 148.72, and 413.62, respectively. Moreover, these findings indicated that the  $IC_{50}$  values of compounds against normal liver cells were very high in comparison to their  $IC_{50}$  doses against the cancer cell lines (Table 3).

### 2.2.3 | Caspase-3 activation assay

Caspase-3 activation for the most active anticancer derivatives **8**, **11** and compound **5** was evaluated. As caspase-3 plays a major role in apoptosis process,<sup>[41]</sup> the obtained results are shown in Figure 2. All the three derivatives activated caspase-3 with a percent exceeding that of thalidomide (30%). Compounds **8** and **11** revealed activation percent at 58 and 64.5%, respectively, followed by compound **5**

activation percent at 47.5%. The obtained results prove the ability of these new derivatives to act as apoptosis inducers, hence good and promising anticancer active agents.

### 2.2.4 | Bcl-2 evaluation

Bcl-2 proteins have been previously reported as an essential factor for apoptosis resistance in hepatocellular carcinoma, additionally, Bcl-2 inhibited apoptosis and promoted the process of tumorigenesis and chemoresistance.<sup>[42]</sup> Results in Figure 3 revealed that the treatment of HepG2 cells with compounds **5**, **8**, **11**, and thalidomide significantly ( $P < 0.001$ ) reduced the expression levels of the anti-apoptotic protein Bcl-2 by 62.76, 76.21, 68.54, and 75.77%, respectively, compared to

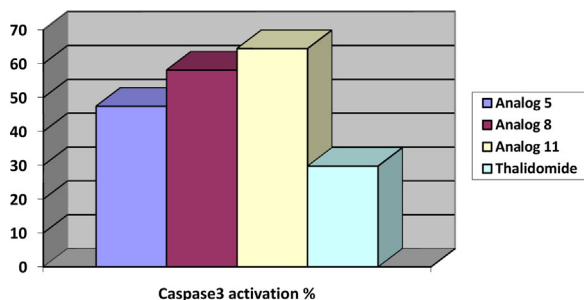
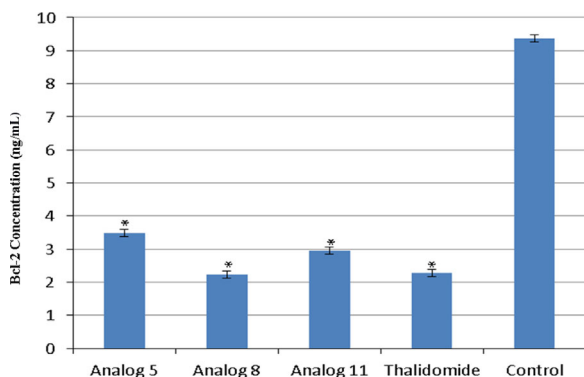
**TABLE 2** Anticancer activity of phthalimide analogs on different human cancer cells

Analog	$IC_{50}$ ( $\mu M$ ) <sup>a</sup>				
	HepG2	MCF-7	A549	H1299	Caco2
2	>200	>200	69.002 ± 2.64	87.074 ± 3.68	93.317 ± 3.76
3	74.13 ± 3.02	>200	100.83 ± 3	69.102 ± 2.79	86.06 ± 3.53
4	78.59 ± 3.32	81.75 ± 3.23	59.93 ± 2.46	64.4 ± 2.76	77.28 ± 2.98
5	69.62 ± 2.88	144.38 ± 5.43	83.24 ± 3.44	55.09 ± 1.59	84.75 ± 3.54
6	123.65 ± 5.04	79.72 ± 3.34	58.06 ± 2.34	46.63 ± 1.32	107.7 ± 3.99
7	63.41 ± 2.55	61.319 ± 1.78	>200	65.75 ± 2.81	54.53 ± 1.69
8	61.67 ± 2.34	62.93 ± 2.54	38.51 ± 0.99	48.83 ± 1.44	58.15 ± 2.36
9	53.34 ± 1.53	108.85 ± 4.05	68.8 ± 2.76	79.25 ± 3.2	60.96 ± 2.79
10	59.37 ± 2.45	78.19 ± 3.15	28.59 ± 0.54	59.62 ± 2.53	56.44 ± 1.87
11	57.38 ± 1.73	106.49 ± 3.89	41.33 ± 1.23	40.85 ± 1.2	49.6 ± 1.54
Thalidomide	193.63 ± 10.04	65.83 ± 2.78	44.53 ± 1.32	52.67 ± 1.43	88.68 ± 3.9

<sup>a</sup> $IC_{50}$  values are the mean ± SD of three independent experiments.

**TABLE 3** Effect of the new promising compounds **5**, **8**, **11**, and thalidomide on normal human liver cells (THLE-2)

Analog	IC <sub>50</sub> (μM) ± SD
	THLE-2
<b>5</b>	951.27 ± 52.06
<b>8</b>	148.72 ± 9.06
<b>11</b>	413.62 ± 15.34
Thalidomide	1598.66 ± 57.24

**FIGURE 2** Caspase-3 activation % for the new compounds and thalidomide**FIGURE 3** Effect of compounds **5**, **8**, **11**, and thalidomide on the expression levels of Bcl-2 in HepG2 cancer cells treated with the compounds at their IC<sub>50</sub> concentrations. Data are expressed as the mean ± SD of three separate experiments. \*Significantly different from control at  $P < 0.001$ 

the control untreated cells (Figure 3). The ability of the tested compounds to significantly down-regulate Bcl-2 levels indicates their potential to enhance apoptosis.

### 2.2.5 | Anti-hepatic fibrosis evaluation

The effect of analogs **5**, **8**, and **11** in a model of liver fibrosis induced in mice by carbon tetrachloride (CCl<sub>4</sub>) action was histopathologically investigated using hematoxylin and eosin (H&E) staining. As shown in Figure 4A and B, liver slides of normal mice showed regular lobulation, central veins, and structures of the portal area. Conversely, liver

slides of fibrotic mice revealed congestion and multifocal interstitial lymphocytic aggregates (Figure 4C) as well as inflammatory cells aggregation in portal area and fibroblastic proliferation. Additionally, marked hydropic degeneration was shown in the surrounding hepatic parenchyma (Figure 4D). Thalidomide-treated mice indicated highly dilated hepatic veins and cystically dilated bile ducts surrounded by fibroblastic proliferation (Figure 4E) as well as telangiectatic sinusoids and mitotically active hepatocytes (Figure 4F). The histopathology of mice treated with analog **11** showed that the central veins and the main hepatic vein radicals were severely dilated and some of them are free of blood others engorged with erythrocytes with a ruptured walls and parenchymal hemorrhage as presented in Figure 4G. Moreover, they showed apparently normal hepatic parenchyma, hypertrophic Kupffer cells, and mitotically active hepatocytes with bluish-red cytoplasm, enlarged nuclei, and double nucleation (Figure 4H). Figure 4I indicated that mice treated with analog **5** revealed apparently normal hepatic parenchyma, mild portal inflammatory reaction, dilated hepatic venous branches, and cystified bile duct. Also, they showed central vein and hepatic sinusoids with normal shapes and structures. Additionally, the hepatocytes are in a good healthy condition with preserved cytoplasm and active prominent nuclei as well as the Kupffer cells are hypertrophied as shown in Figure 4J. The treatment with analog **8** presented apparently normal hepatic parenchyma and vascular tree with preserved biliary and lymphatic structures and minimal portal inflammatory reactions. Moreover, most of hepatocytes are highly activated with prominent enlarged hyperchromatic nuclei as well as the Kupffer cells are moderately hypertrophied and showed preserved normal morph-histology structures (Figure 4K and L).

### 2.3 | Molecular docking studies

Results showed that analog **8** exhibited a broad spectrum activity. So that, these results motivated us to investigate its binding mode and possible interaction with topoisomerase II DNA gyrase. The co-crystallized ligand (clorobiocin) was redocked into the pocket site of topoisomerase II DNA. It showed a docking score energy  $-14.5$  kcal/mol at root mean square deviation (RMSD) value equal 1.2. Also, it has formed three hydrogen bonding with Arg 136, Asn 46, and Asp 73 in addition to arene-cation interaction with Arg 76 amino acid as shown in Figure 5. Compound **8** was drawn in 2D then transformed to 3D, energy minimized and saved in a molecular data base (MDB) file to be docked into the active site of topoisomerase II DNA enzyme. It showed score energy lower than the co-crystallized ligand ( $-16.4$  kcal/mol) with two arene-cation interactions with Arg 76 amino acid through its indole moiety (Figure 6). Additional investigations for affinity, binding mode, and possible interactions of the promising new derivatives **5** and **11** were also performed, their docking score energy was  $-8.2$  and  $-10.01$  kcal/mol, respectively, they showed less binding affinity than compound **8**, this might help in explaining why activity of compound **8** is better. Figures 7 and 8 represented their binding and interactions with topoisomerase II DNA binding site. Both of them **5** and **11** showed one arene-cation interaction with Arg 76 amino acid, and both showed ligand exposure through the phenyl and alkyl

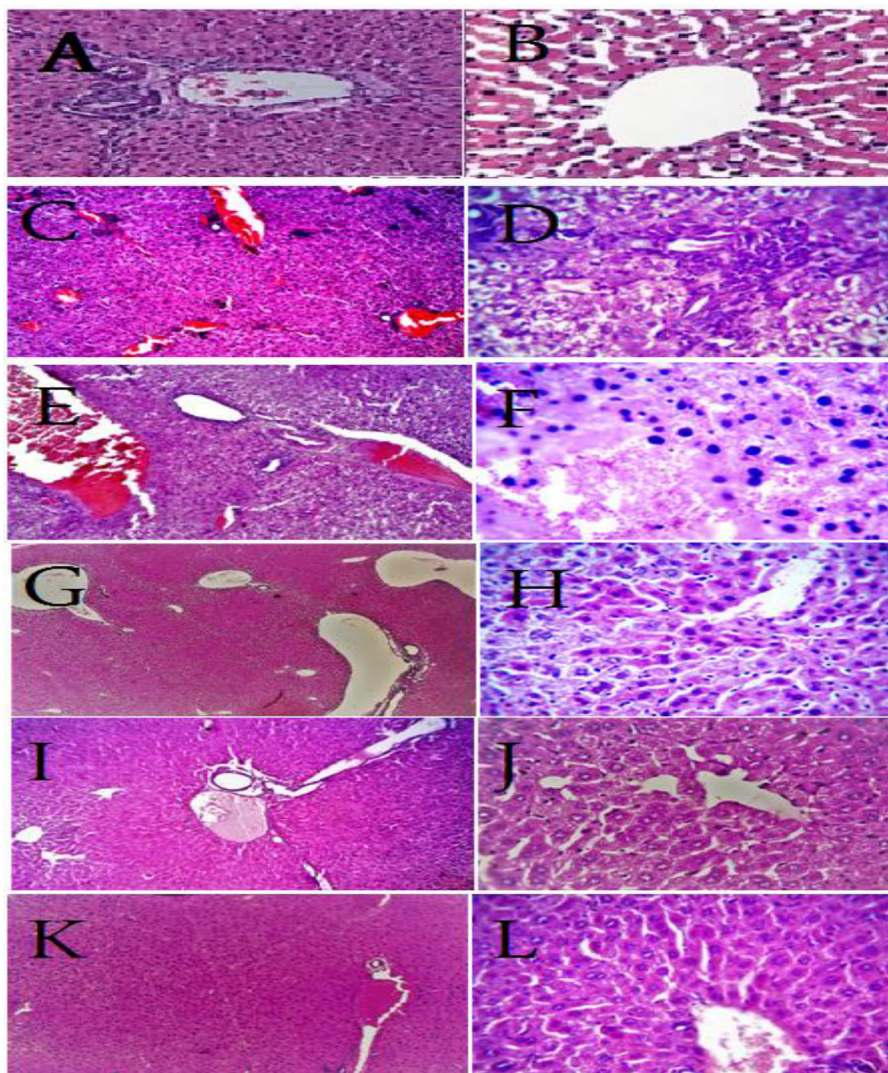


**FIGURE 4** Histopathological analysis of liver tissues: (A and B) Liver section of normal group observed under microscope (100 and 400, respectively); (C and D) liver section of  $\text{CCl}_4$  control observed under microscope (100 and 400, respectively); (E and F) liver section of  $\text{CCl}_4$  + thalidomide observed under microscope (100 and 400, respectively); (G and H) liver section of  $\text{CCl}_4$  + analog **11** observed under microscope (100 and 400, respectively); (I and J) liver section of  $\text{CCl}_4$  + analog **5** observed under microscope (100 and 400, respectively); (K and L) liver section of  $\text{CCl}_4$  + analog **8** observed under microscope (100 and 400, respectively)

derivative as shown in the 2D interaction figures, compound **11** with lower docking score energy and with additional ligand exposure with the receptor through its Br atom as like as compound **8**. These results are in agreement with the biological screening results as compound **8** was the best active one of them, followed by compound **11**, then compound **5**.

## 2.4 | Structure–activity relationship (SAR)

It is noticed that the R group and Br atom affected the antimicrobial activity of the synthesized compounds. Concerning *B. subtilis*, derivatives containing allyl **5** and *n*-propyl **6** groups are the most active antibacterial analogs. Bromination decreases their activity against such gram positive bacteria. Analog containing benzyl group **4** and the brominated analog **8** have the highest antibacterial activity

against *S. aureus*. Bromination of derivative **3** increased its activity against *E. coli* while decreased the antibacterial activity of the other analogs against the same bacteria. The effect of allyl and *n*-propyl groups appears again in the activity of derivatives **5** and **6**, they showed the highest activity against *P. aeruginosa*. The brominated derivative **8** showed higher activity against the same bacteria than the non-brominated one **3**. As for *C. albicans*, the brominated derivatives **10** and **11** exhibited the highest antifungal activity, these compounds have allyl and *n*-propyl groups, respectively. The brominated derivatives **8**, **10**, and **11** are the best antifungal active agents against *Asp. niger*. Derivative **8** has the highest antimicrobial activity against five types of microorganisms, so this attracts us to investigate more about such compound. The linker between phthalimide and indole moieties might have an important role in the anticancer activity of the synthesized compounds. This appears clearly against HepG2 and Caco2 cells.

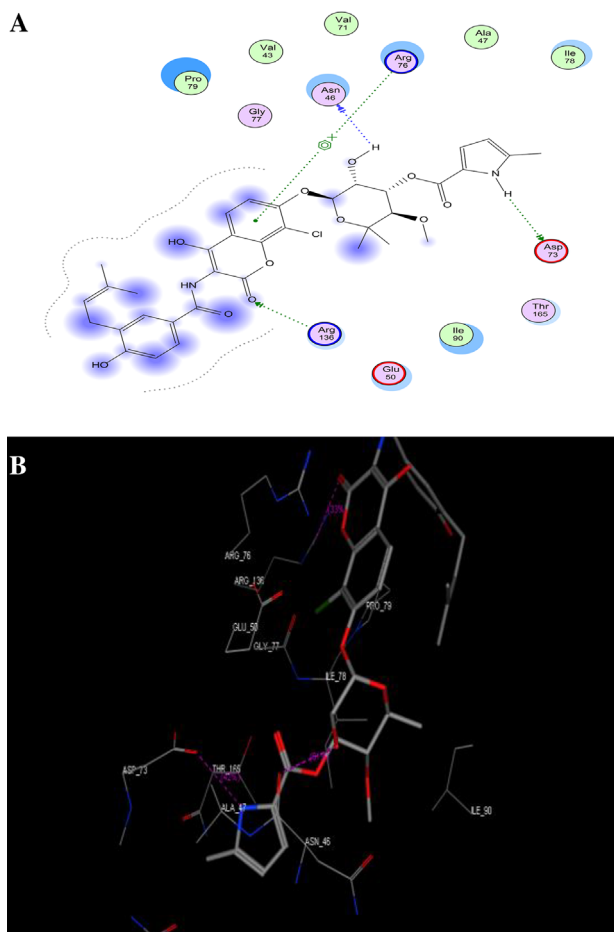


**FIGURE 5** (A) 2D interactions for the co-crystallized ligand (clorobiocin) in the binding site of topoisomerase II DNA gyrase. (B) 3D interactions for the co-crystallized ligand (clorobiocin) in the binding site of topoisomerase II DNA gyrase

Except derivative **2**, all tested compounds are more potent than thalidomide, which does not have a linker, against HepG2 cells. Among the non-brominated compounds, compound **5**, containing unsaturated allyl substituent, has the most potency against HepG2 cells ( $IC_{50} = 69.617 \mu M$ ). Compound **6**, containing the saturated *n*-propyl group, has the lowest potency. Bromination increases the potency of the compounds against liver carcinoma cells. These data support the synthesis of potent anti-liver cancer compounds containing spacer attached to phthalimide moiety in the future. Bromination increases the cytotoxicity of the analogs, except for analogs **4** and **6**, against MCF-7 cancer cells. Introduction of Br atom increases the anticancer activity of the derivatives, except for **2** and **4**, toward A549 cells. Saturated *n*-propyl group might have a role in the potency of the derivatives against H1299 cells. Derivatives **6** and **11** have the lowest  $IC_{50}$  values (46.631 and 40.847  $\mu M$ , respectively). The brominated derivative **8** is more potent than its non-brominated analog **3** against H1299. Regarding Caco2 cells, bromination increases the cytotoxicity of the compounds. This suggests that Br atom might have a role in the cytotoxicity against Caco2 cells. So, brominated indole scaffolds can be taken in consideration in the future to build up new cytotoxic

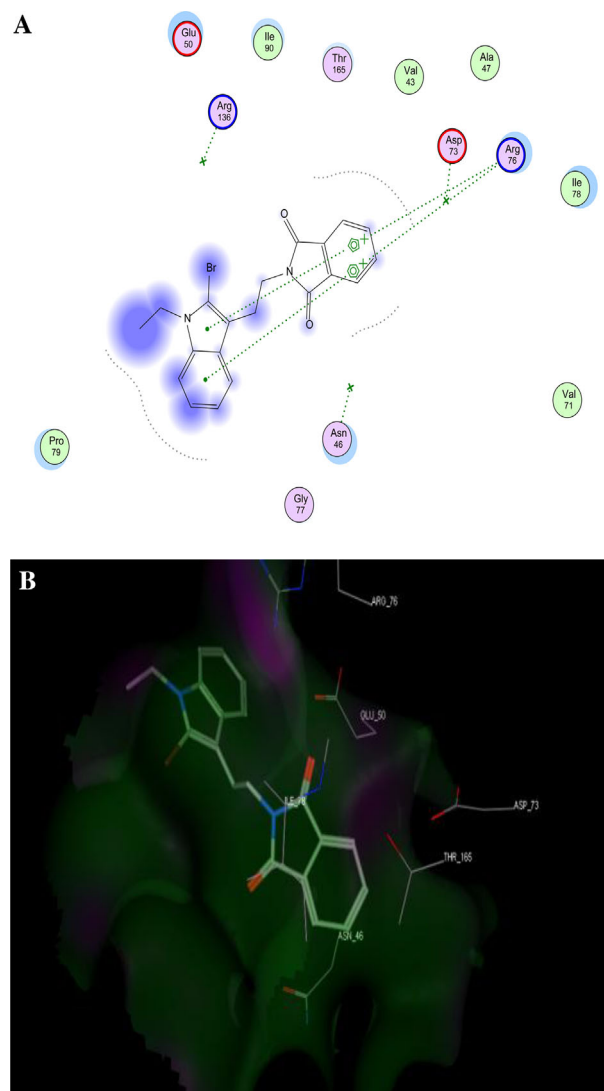


**FIGURE 6** (A) 2D interactions of analog **8** with topoisomerase II DNA gyrase binding sites. (B) 3D interactions of analog **8** with topoisomerase II DNA gyrase binding sites

compounds against Caco2 cancer cells. The brominated derivative **8** is more potent than the drug thalidomide against all tested cancer cell lines. The potency of the brominated derivative **11** is higher than that of thalidomide against HepG2, A549, H1299, and Caco2 cell lines. These two compounds **8** and **11** attract us to understand more about their activity.

### 3 | CONCLUSION

A series of novel thalidomide analogs were synthesized. Compound **8** showed a broad spectrum antimicrobial activity. The new analogs exhibited anticancer activity toward different cancer cell lines, especially HepG2 and Caco2 cancer cells. Compounds **8** and **11** showed to be the best active analogs as anticancer agents. Caspase-3 activation for these compounds (58 and 64.5%) was much better than for thalidomide (30%) and compound **5** (47.5%) that showed to be

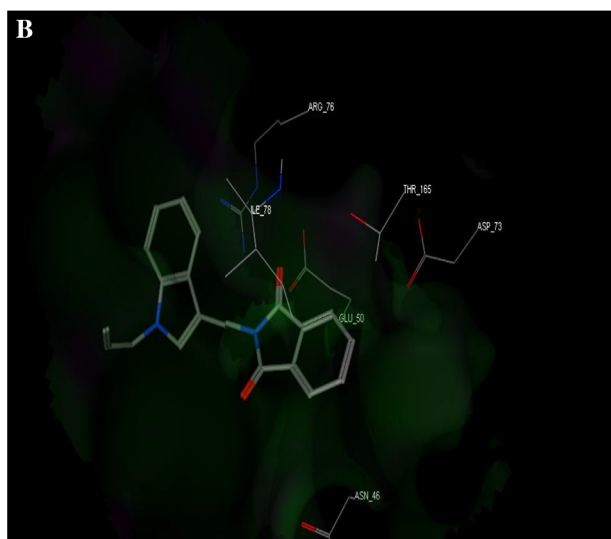
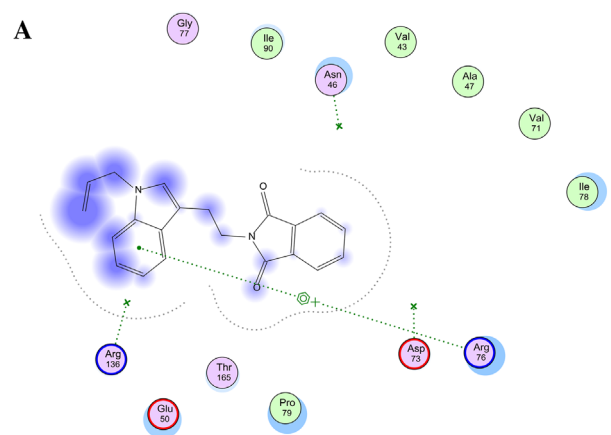


**FIGURE 7** (A) 2D interactions of analog **5** with topoisomerase II DNA gyrase binding sites. (B) 3D interactions of analog **5** with topoisomerase II DNA gyrase binding sites

active on two cancer cell lines only. Furthermore, compound **8** and thalidomide inhibited the Bcl-2 concentration level (76.21 and 75.77%) followed by compound **11** (68.54%) and compound **5** (62.76%). Moreover, compound **8** improved the fibrotic liver tissues to normal ones. Further investigations are recommended especially on analogs **8** and **11** as they are promising candidates with potential anticancer activity.

## 4 | EXPERIMENTAL

### 4.1 | Chemistry

#### 4.1.1 | General

Melting points for the synthesized compounds were measured using a Stuart melting point apparatus and are uncorrected. The reaction progress was monitored using TLC aluminum sheets silica gel (Merck 60F<sub>254</sub>) and visualized using UV lamp. The <sup>1</sup>H NMR spectra for all new derivatives were recorded on Varian Gemini NMR spectrometer in

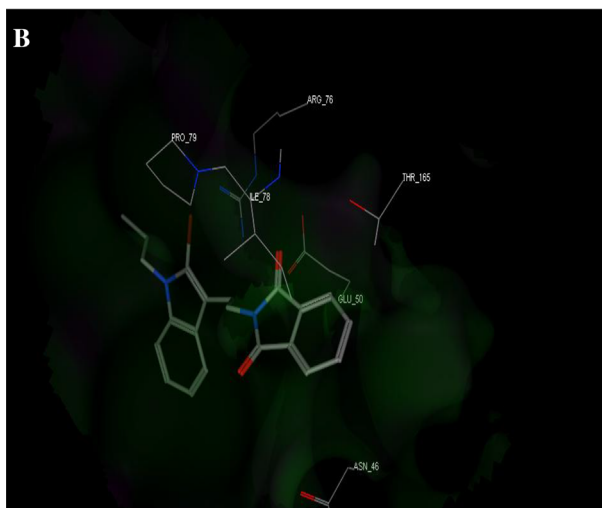
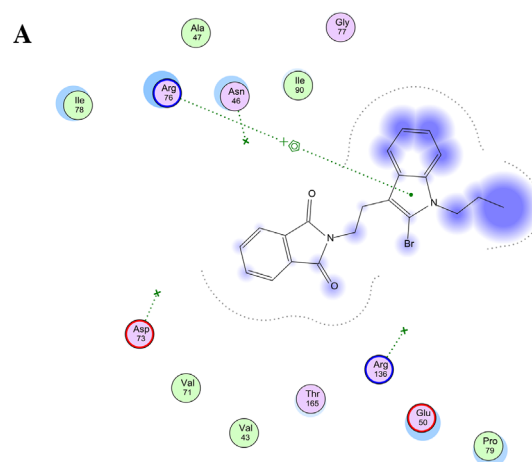


**FIGURE 8** (A) 2D interactions of analog **11** with topoisomerase II DNA gyrase binding sites. (B) 3D interactions of analog **11** with topoisomerase II DNA gyrase binding sites

DMSO-*d*<sub>6</sub> as solvent at 300 MHz using TMS as internal standard and the chemical shifts were reported as  $\delta$  values in ppm. The <sup>13</sup>C NMR spectra for synthesized compounds **5**, **6**, **8**, and **11** were recorded on a Bruker 400 MHz (Ulm University, Germany) in DMSO-*d*<sub>6</sub> as solvent at 101 MHz, while the <sup>13</sup>C NMR spectra for the compounds **7**, **9**, and **10** were recorded on JEOL JNM-ECZ500R-500 MHz (Mansoura University, Egypt) in DMSO-*d*<sub>6</sub> as solvent at 400 MHz using TMS as internal standard and the chemical shifts were reported as  $\delta$  values in ppm. Mass spectra were recorded with a Shimadzu QP-2010 Plus mass spectrometer in EI (70 eV) mode. The elemental analyses were performed at the Micro Analytical Center, Cairo University, Egypt.

The NMR spectra as well as the InChI codes together with some biological activity data are provided as Supporting Information.

#### 4.1.2 | General procedure for the synthesis of isoindole derivatives 2–6

To a solution of isoindole **1** (1 mmol) in dry DMF (3 mL), sodium hydride (NaH) (1.5 mmol) was added, and kept stirring at room temperature for

30 min, then the appropriate halide derivative (1.5 mmol) was added dropwise. The reaction mixture was heated under reflux for 1 h. After completion of the reaction as monitored by TLC, the reaction was diluted with water and the product was extracted with diethyl ether. The organic layer was dried over anhydrous  $\text{Na}_2\text{SO}_4$ , filtered off, and concentrated to give a residue, which was purified by column chromatography on silica gel to afford the isoindole derivatives 2–6.

#### 2-[2-[1-(Prop-2-en-1-yl)-1H-indol-3-yl]ethyl]-1H-isoindole-1,3(2H)-dione (5)

Greenish-yellow crystals; m.p. 126–128°C; yield: 52%;  $^1\text{H}$  NMR (DMSO- $d_6$ , 300 MHz),  $\delta$  ppm: 3.03 (t,  $J = 7.8$  Hz, 2H), 3.85 (t,  $J = 7.8$  Hz, 2H), 4.72 (d,  $J = 5.1$  Hz, 2H), 4.90 (d,  $J = 17.1$  Hz, 1H), 5.04 (d,  $J = 10.2$  Hz, 1H), 5.86–5.92 (m, 1H), 6.99 (t,  $J = 7.5$  Hz, 1H), 7.10 (t,  $J = 8.1$  Hz, 1H), 7.14 (s, 1H), 7.35 (d,  $J = 7.8$  Hz, 1H), 7.58 (d,  $J = 7.2$  Hz, 1H), 7.83–7.84 (m, 4H).  $^{13}\text{C}$  NMR (DMSO- $d_6$ , 101 MHz, ppm):  $\delta$  23.60, 38.18, 47.67, 109.93, 110.36, 116.20, 118.29, 118.55, 121.14, 122.91, 126.46, 127.48, 131.57, 134.29, 134.36, 136.01, 167.71. MS ( $m/z$ , relative abundance %): 331 ( $\text{M}^+ + 1$ , 25), 330 ( $\text{M}^+$ , 100). Anal. calcd. for  $\text{C}_{21}\text{H}_{18}\text{N}_2\text{O}_2$ : C, 76.34; H, 5.49; N, 8.48. Found: C, 76.49; H, 5.87; N, 8.60.

#### 2-[2-(1-Propyl-1H-indol-3-yl)ethyl]-1H-isoindole-1,3(2H)-dione (6)

Green crystals; m.p. 110–112°C; yield: 65%;  $^1\text{H}$  NMR (DMSO- $d_6$ , 300 MHz),  $\delta$  ppm: 0.72 (t,  $J = 7.5$  Hz, 3H), 1.63–1.70 (m, 2H), 3.03 (t,  $J = 7.5$  Hz, 2H), 3.84 (t,  $J = 7.5$  Hz, 2H), 4.03 (t,  $J = 6.9$  Hz, 2H), 6.99 (t,  $J = 7.8$  Hz, 1H), 7.10 (t,  $J = 7.2$  Hz, 1H), 7.16 (s, 1H), 7.38 (d,  $J = 7.5$  Hz, 1H), 7.55 (d,  $J = 6.9$  Hz, 1H), 7.8–7.86 (m, 4H).  $^{13}\text{C}$  NMR (DMSO- $d_6$ , 101 MHz, ppm):  $\delta$  11.03, 23.05, 23.61, 38.19, 46.74, 109.74, 109.85, 118.29, 118.34, 120.99, 122.92, 126.44, 127.38, 131.58, 134.29, 136.02, 167.74. MS ( $m/z$ , relative abundance %): 333 ( $\text{M}^+ + 1$ , 25), 332 ( $\text{M}^+$ , 100). Anal. calcd. for  $\text{C}_{21}\text{H}_{20}\text{N}_2\text{O}_2$ : C, 75.88; H, 6.06; N, 8.43. Found: C, 75.60; H, 5.81; N, 8.38.

### 4.1.3 | General procedure for the synthesis of isoindole derivatives 7–11

To a suspension of isoindole derivatives 2–6 (1 mmol) in  $\text{CCl}_4$  (5 mL), *N*-bromosuccinimide (NBS) (1.5 mmol) was added. The reaction mixture was stirred at reflux for 1 h and monitored by TLC. After completion of the reaction, the precipitate was filtered off to remove the unreacted NBS. The solvent was evaporated under reduced pressure and the residue was recrystallized from ethanol to afford the isoindole derivatives 7–11.

#### 2-[2-(2-Bromo-1-methyl-1H-indol-3-yl)ethyl]-1H-isoindole-1,3(2H)-dione (7)

Yellow solids; m.p. 162–164°C; yield: 60%;  $^1\text{H}$  NMR (DMSO- $d_6$ , 300 MHz),  $\delta$  ppm: 3.03 (t,  $J = 6.9$  Hz, 2H), 3.69 (s, 3H), 3.78 (t,  $J = 7.5$  Hz, 2H), 7.02 (t,  $J = 7.5$  Hz, 1H), 7.14 (t,  $J = 7.8$  Hz, 1H), 7.44 (d,  $J = 8.1$  Hz, 1H), 7.53 (d,  $J = 7.2$  Hz, 1H), 7.81–7.82 (m, 4H).  $^{13}\text{C}$  NMR (DMSO- $d_6$ , 500 MHz, ppm):  $\delta$  23.86, 31.35, 37.22, 10.09, 110.45, 113.55, 117.46,

119.51, 121.72, 122.96, 126.51, 131.57, 134.34, 136.52, 167.71. MS ( $m/z$ , relative abundance %): 384 ( $\text{M}^+ + 2$ , 4), 382 ( $\text{M}^+$ , 4). Anal. calcd. for  $\text{C}_{19}\text{H}_{15}\text{BrN}_2\text{O}_2$ : C, 59.55; H, 3.95; N, 7.31. Found: C, 59.71; H, 3.67; N, 7.41.

#### 2-[2-(2-Bromo-1-ethyl-1H-indol-3-yl)ethyl]-1H-isoindole-1,3(2H)-dione (8)

Pale yellow solids; m.p. 127–129°C; yield: 70%;  $^1\text{H}$  NMR (DMSO- $d_6$ , 300 MHz),  $\delta$  ppm: 1.13 (t,  $J = 7.2$  Hz, 3H), 3.02 (t,  $J = 7.2$  Hz, 2H), 3.79 (t,  $J = 6.9$  Hz, 2H), 4.19 (q,  $J = 6.9$  Hz, 2H), 7.02 (t,  $J = 7.2$  Hz, 1H), 7.13 (t,  $J = 7.2$  Hz, 1H), 7.46 (d,  $J = 8.4$  Hz, 1H), 7.54 (d,  $J = 8.1$  Hz, 1H), 7.81 (s, 4H).  $^{13}\text{C}$  NMR (DMSO- $d_6$ , 101 MHz, ppm):  $\delta$  14.73, 23.74, 37.13, 39.49, 109.84, 110.76, 112.32, 117.59, 119.43, 121.67, 122.81, 126.81, 131.55, 134.23, 135.43, 167.56. MS ( $m/z$ , relative abundance %): 398 ( $\text{M}^+ + 2$ , 15), 396 ( $\text{M}^+$ , 15). Anal. calcd. for  $\text{C}_{20}\text{H}_{17}\text{BrN}_2\text{O}_2$ : C, 60.47; H, 4.31; N, 7.05. Found: C, 59.94; H, 4.00; N, 7.23.

#### 2-[2-(1-Benzyl-2-bromo-1H-indol-3-yl)ethyl]-1H-isoindole-1,3(2H)-dione (9)

White solids; m.p. 129–131°C; yield: 80%;  $^1\text{H}$  NMR (DMSO- $d_6$ , 300 MHz),  $\delta$  ppm: 3.09 (t,  $J = 6.6$  Hz, 2H), 3.85 (t,  $J = 6.6$  Hz, 2H), 5.41 (s, 2H), 6.92 (d,  $J = 6.9$  Hz, 1H), 7.06–7.12 (m, 3H), 7.19–7.28 (m, 3H), 7.37 (d,  $J = 8.1$  Hz, 1H), 7.58 (d,  $J = 7.2$  Hz, 1H), 7.79 (s, 4H).  $^{13}\text{C}$  NMR (DMSO- $d_6$ , 500 MHz, ppm):  $\delta$  23.80, 37.22, 47.28, 110.36, 111.32, 113.41, 117.79, 119.78, 122.00, 122.93, 126.00, 126.88, 127.11, 128.52, 131.54, 134.30, 136.17, 137.44, 167.71. MS ( $m/z$ , relative abundance %): 460 ( $\text{M}^+ + 2$ , 1), 458 ( $\text{M}^+$ , 1). Anal. calcd. for  $\text{C}_{25}\text{H}_{19}\text{BrN}_2\text{O}_2$ : C, 65.37; H, 4.17; N, 6.10. Found: C, 65.16; H, 3.85; N, 6.22.

#### 2-[2-[2-Bromo-1-(prop-2-en-1-yl)-1H-indol-3-yl]ethyl]-1H-isoindole-1,3(2H)-dione (10)

Yellow solids; m.p. 145–147°C; yield: 65%;  $^1\text{H}$  NMR (DMSO- $d_6$ , 300 MHz),  $\delta$  ppm: 3.05 (t,  $J = 7.2$  Hz, 2H), 3.82 (t,  $J = 6.9$  Hz, 2H), 4.56 (d,  $J = 17.1$  Hz, 1H), 4.77 (d,  $J = 4.5$  Hz, 2H), 4.99 (d,  $J = 10.2$  Hz, 1H), 5.79–5.85 (m, 1H), 7.02 (t,  $J = 7.8$  Hz, 1H), 7.12 (t,  $J = 8.4$  Hz, 1H), 7.39 (d,  $J = 7.8$  Hz, 1H), 7.55 (d,  $J = 7.8$  Hz, 1H), 7.79 (s, 4H).  $^{13}\text{C}$  NMR (DMSO- $d_6$ , 500 MHz, ppm):  $\delta$  23.79, 37.18, 46.23, 110.19, 110.99, 113.11, 115.65, 117.68, 119.65, 121.85, 122.91, 126.70, 131.57, 133.21, 134.30, 136.00, 167.69. MS ( $m/z$ , relative abundance %): 410 ( $\text{M}^+ + 2$ , 2), 408 ( $\text{M}^+$ , 2). Anal. calcd. for  $\text{C}_{21}\text{H}_{17}\text{BrN}_2\text{O}_2$ : C, 61.63; H, 4.19; N, 6.84. Found: C, 61.32; H, 3.93; N, 6.75.

#### 2-[2-(2-Bromo-1-propyl-1H-indol-3-yl)ethyl]-1H-isoindole-1,3(2H)-dione (11)

White solids; m.p. 101–103°C; yield: 75%;  $^1\text{H}$  NMR (DMSO- $d_6$ , 300 MHz),  $\delta$  ppm: 0.74 (t,  $J = 7.8$  Hz, 3H), 1.57–1.62 (m, 2H), 3.04 (t,  $J = 7.2$  Hz, 2H), 3.81 (t,  $J = 6.9$  Hz, 2H), 4.09 (t,  $J = 7.5$  Hz, 2H), 7.01 (t,  $J = 7.8$  Hz, 1H), 7.13 (t,  $J = 8.1$  Hz, 1H), 7.46 (d,  $J = 8.1$  Hz, 1H), 7.53 (d,  $J = 7.8$  Hz, 1H), 7.77–7.80 (m, 4H).  $^{13}\text{C}$  NMR (DMSO- $d_6$ , 101 MHz, ppm):  $\delta$  10.76, 22.70, 23.75, 37.15, 45.58, 110.10, 110.62, 112.91, 117.58, 119.39, 121.62, 122.83, 126.63, 131.56, 134.23, 136.01, 167.59. MS ( $m/z$ , relative abundance %): 412 ( $\text{M}^+ + 2$ , 4), 410 ( $\text{M}^+$ , 4).

Anal. calcd. for  $C_{21}H_{19}BrN_2O_2$ : C, 61.33; H, 4.66; N, 6.81. Found: C, 61.62; H, 4.88; N, 6.60.

## 4.2 | Biological assays

### 4.2.1 | Antimicrobial activity

The antimicrobial activity was performed using the agar diffusion technique.<sup>[43]</sup> All examinations were done in duplicates against gram positive bacteria (*B. subtilis* ATCC 6633, *S. aureus* ATCC 35556), gram negative bacteria (*E. coli* ATCC 23282 and *P. aeruginosa* ATCC 10145), fungi (*C. albicans* IMRU 3669) and filamentous fungus (*Asp. niger* ATCC 16404). The bacteria were grown on nutrient agar while the fungi were grown on Czapek's Dox agar medium. The bacteria and fungi were exposed to 5 mg/mL of each analog for 24 and 48 h, respectively. Erythromycin was used as positive control for bacteria and miconazole for fungi.

### 4.2.2 | Anticancer activity method

The five cell lines, mammary gland breast cancer cell line (MCF-7), human intestinal cancer cells (Caco2), human hepatocellular carcinoma cell line (HepG2) and human lung cancer cells (H1299 and A549) were obtained from VACSERA-Cell Culture Unit, Cairo, Egypt. The cells were cultured in RPMI-1640 medium with 10% fetal bovine serum. Antibiotics were added (100 units/mL penicillin and 100 µg/mL streptomycin) at 37°C in a 5% CO<sub>2</sub> incubator.

The cells were seeded in a 96-well plate at a density of 10<sup>4</sup> cells/well for 48 h at 37°C under 5% CO<sub>2</sub>. After incubation, the cells were treated with phthalimide analogs in a range of concentration (6.25–200 µM) and incubated for 24 h, then the medium was discarded. Fix with 10% trichloroacetic acid (TCA) 150 µL/well for 1 h at 4°C. Wash by water three times (TCA reduce SRB protein binding). Wells were stained by SRB 70 µL/well for 10 min at room temperature with 0.4%. Wash with acetic acid 1% to remove unbound dye. The plates will be 24 h air dried. The dye will be solubilized with 50 µL/well of 10 mM Tris base (pH 7.4) for 5 min on a shaker at 1600 rpm. The optical density (OD) of each well was measured at 570 nm with an ELISA microplate reader (EXL 800 USA). The relative cell viability in percentage was calculated as  $(A_{570} \text{ of treated samples} / A_{570} \text{ of untreated sample}) \times 100$  and the IC<sub>50</sub> values were calculated using sigmoidal concentration response curve fitting models (SigmaPlot software).

### 4.2.3 | Caspase-3 activation assay

After treating the HepG2 cells with selected compounds for 48 h, harvested cells were lysed with caspase lysis buffer at pH 7.5 and then incubated with Ac-DEVD-AMC/Ac-LEHD-AFC substrate in 20 mM HEPES (pH 7.5), 0.1% CHAPS, 2 mM EDTA, and 5 mM DTT at 37°C for 2 h. The released AMC and AFC are directly proportional to caspase-3 activity, they were detected at wavelength of 380/460 nm (for AMC), 400/505 nm (for AFC). The obtained values were normalized with total protein concentration and the relative

caspase activity were calculated as the ratio of values between mock treated and treated cells.<sup>[44]</sup>

### 4.2.4 | Bcl-2 assay

HepG2 cells (ATCC) were seeded in a 96-well plate at density  $1.8 \times 10000$  cells/well in RPMI 1640 containing 10% fetal bovine serum. Cells were incubated for overnight and then the culture medium was replaced with fresh medium (100 µL) and cells were treated with the tested compounds at their IC<sub>50</sub> values and incubated at 37°C for 24 h. After incubation period, cells were lysed with cell extraction buffer and then the lysates were diluted in standard diluent buffer. Bcl-2 concentration was measured using ELISA kit (Invitrogen Zymed® Bcl-2 ELISA Kit (96 tests) according to the supplier's protocol. The Bcl-2 concentrations (ng/mL) in cell lysates were obtained from the constructed standard curve. The experiment was repeated three independent times and the concentration of Bcl-2 were expressed as mean ± SD.

### 4.2.5 | In vivo liver fibrosis model

#### Experimental animals

Sixty male albino mice (22 ± 3 g) were obtained from National Research Centre (Cairo, Egypt). The mice were selected for the study and maintained at a controlled temperature of 25°C and constant humidity (50–70%) under a 12-h light/dark cycle, with free access to diet and water. The animal study was performed according to the international rules considering animal experiments and the internationally accepted ethical principles for laboratory animal use and care.

#### Experimental design for antifibrotic activity

Liver fibrosis was induced in male albino mice by intraperitoneal injection (IP) of CCl<sub>4</sub> at a dose of 0.4 mL/kg dissolved in olive oil twice a week for 8 weeks. All the groups were injected with CCl<sub>4</sub> except group 1 (negative control group) animals were taken olive oil twice a week for 8 weeks. Eight weeks after fibrosis induction male albino mice were divided into five groups (10 mice each) and treated with 10 mg/kg of analogs **5**, **8**, and **11** once daily for 8 weeks. At the end of the study, the animals were anesthetized with ether and sacrificed. Liver tissues of all animals were removed and stored in –80°C in nuclease free tubes for the histopathological analysis.

#### Histopathological examination

The formalin preserved hepatic tissues of the tested mice were processed in an automated tissue processor. The processing consisted of an initial two steps fixation and dehydration. Fixation comprising tissue immersion in 10% buffered formalin for 48 h, followed by removal of fixative in distilled water for 30 min. Dehydration was then carried out by running the tissues through a graded series of alcohol (70, 90, and 100%). The tissue was initially exposed to 70% alcohol for 120 min followed by 90% alcohol for

90 min and then two cycles of absolute alcohol, each for 1 h. Dehydration was then followed by clearing the samples in several changes of xylene. It consisted of tissue immersion for an hour in a mixture comprising 50% alcohol and 50% xylene, followed by pure xylene for one and a half hour. Samples were then impregnated with molten paraffin wax, then embedded and blocked out. Paraffin sections (4–5 µm) were stained with hematoxylin and eosin and then examined for liver fibrosis.

### 4.3 | Molecular docking study

Docking study was performed by downloading the Protein Data Bank (PDB) file: 1KZN,<sup>[45]</sup> refined by removing water molecules then protonated and the pocket was detected using Molecular Operating Environment software 10.2008 (MOE) provided with chemical computing group, Canada. 1KZN represents clorobiocin co-crystallized with topoisomerase II DNA enzyme, verification process was performed by redocking of the co-crystallized ligand into the active site using the default settings 2D of the synthesized derivatives **5**, **8**, and **11** were converted to 3D by ChemDraw, then protonated, energy minimized by Merck Molecular force field (MMff 94x) and saved in an mdb file to be docked into the binding site of the selected enzyme.

### CONFLICT OF INTEREST

The authors declare that there is no conflict of interest.

### ORCID

Amany Belal  <http://orcid.org/0000-0003-1045-0163>

### REFERENCES

- https://www.cancer.org/content/dam/cancer-org/research/cancer-facts-and-statistics/annual-cancer-facts-and-figures/2016/cancer-facts-and-figures-2016.pdf.
- A. Kamal, G. B. Kumar, V. L. Nayak, V. S. Reddy, A. B. Shaik, Rajender, M. K. Reddy, *MedChemComm* **2015**, *6*, 606.
- Y. Hashimoto, *Arch. Pharm. Chem. Life Sci.* **2008**, *341*, 536.
- C. Shinji, T. Nakamura, S. Maeda, M. Yoshida, Y. Hashimoto, H. Miyachi, *Bioorg. Med. Chem. Lett.* **2005**, *15*, 4427.
- F. Wang, H. Yin, C. Yue, S. Cheng, M. Hong, *J. Organomet. Chem.* **2013**, *738*, 35.
- W. Si, T. Zhang, L. Zhang, X. Mei, M. Dong, K. Zhang, J. Ning, *Bioorg. Med. Chem. Lett.* **2016**, *26*, 2380.
- P. F. Lamie, J. N. Philoppes, A. O. El-Gendy, L. Rarova, J. Gruz, *Molecules* **2015**, *20*, 16620.
- N. S. El-Gohary, M. I. Shaaban, *Arch. Pharm. Chem. Life Sci.* **2015**, *348*, 666.
- H. E. A. Ahmed, H. A. Abdel-Salam, M. A. Shaker, *Bioorg. Chem.* **2016**, *66*, 1.
- K. M. Amin, A. H. El-masry, N. A. Mohamed, G. E. A. Awad, B. S. Habib, *Der Pharm. Chem.* **2013**, *5*, 97.
- R. Bannela, S. P. Shrivastava, *Chem. Sci. Trans.* **2012**, *1*, 431.
- A. M. Khalil, M. A. Berghot, M. A. Gouda, *Eur. J. Med. Chem.* **2010**, *45*, 1552.
- S. H. L. Kok, R. Gambari, C. H. Chui, M. C. W. Yuen, E. Lin, R. S. M. Wong, F. Y. Lau, G. Y. M. Cheng, W. S. Lam, S. H. Chan, K. H. Lam, C. H. Cheng, P. B. S. Lai, M. W. Y. Yu, F. Cheung, J. C. O. Tang, A. S. C. Chan, *Bioorg. Med. Chem.* **2008**, *16*, 3626.
- S. H. Chan, K. H. Lam, C. H. Chui, R. Gambari, M. C. W. Yuen, R. S. M. Wong, G. Y. M. Cheng, F. Y. Lau, Y. K. Au, C. H. Cheng, P. B. S. Lai, C. W. Kan, S. H. L. Kok, J. C. O. Tang, A. S. C. Chan, *Eur. J. Med. Chem.* **2009**, *44*, 2736.
- T. Noguchi, H. Fujimoto, H. Sano, A. Miyajima, H. Miyachi, Y. Hashimoto, *Bioorg. Med. Chem. Lett.* **2005**, *15*, 5509.
- S. G. Stewart, D. Spagnolo, M. E. Polomska, M. Sin, M. Karimi, L. J. Abraham, *Bioorg. Med. Chem. Lett.* **2007**, *17*, 5819.
- H.-W. Man, P. Schafer, L. M. Wong, R. T. Patterson, L. G. Corral, H. Raymon, K. Blease, J. Leisten, M. A. Shirley, Y. Tang, D. M. Babusis, R. Chen, D. Stirling, G. W. Muller, *J. Med. Chem.* **2009**, *52*, 1522.
- W. N. Brennen, C. R. Cooper, S. Capitosti, M. L. Brown, R. A. Sikes, *Clin. Prostate Cancer* **2004**, *3*, 54.
- R. Kerbel, J. Folkman, *Nat. Rev. Cancer* **2002**, *2*, 727.
- I. Ali, W. A. Wani, K. Saleem, A. Haque, *Curr. Drug Ther.* **2012**, *7*, 13.
- M. A. H. Zahran, Y. G. Abdin, A. M. A. Osman, A. M. Gamal-Eldeen, R. M. Talaat, E. B. Pedersen, *Arch. Pharm. Chem. Life Sci.* **2014**, *347*, 1.
- P. Sharma, A. Kumar, P. Pandey, *Indian J. Chem.* **2006**, *45B*, 2077.
- M. A. H. Zahran, H. F. Salama, Y. G. Abdin, A. M. Gamal-Eldeen, *J. Chem. Sci.* **2010**, *122*, 587.
- P. Çıkla, D. Özsvacı, Ö. B. Özakpınar, A. Şener, Ö. Çevik, S. Ö-Turan, J. Akbuğa, F. Şahin, S. G. Kvcvkgvzel, *Arch. Pharm. Chem. Life Sci.* **2013**, *346*, 367.
- V. Kumar, S. K. Sharma, S. Singh, A. Kumar, S. Sharma, *Arch. Pharm. Chem. Life Sci.* **2010**, *343*, 98.
- a) D. G. Barceloux, *Medical Toxicology of Drug Abuse: Synthesized Chemicals and Psychoactive Plants*. John Wiley & Sons, Inc., Hoboken, NJ, USA **2012**, p. 193; b) A. J. K. Karamyan, M. T. Hamann, *Chem. Rev.* **2010**, *110*, 4489.
- R. F. Salikov, A. Y. Belyy, N. S. Khusnutdinova, Y. V. Vakhitova, Y. V. Tomilov, *Bioorg. Med. Chem. Lett.* **2015**, *25*, 3597.
- J. L. Brandes, D. Kudrow, S. R. Stark, C. P. O'Carroll, J. U. Adelman, F. J. O'Donnell, W. J. Alexander, S. E. Spruill, P. S. Barrett, S. E. Lener, *Am. Med. Assoc.* **2007**, *297*, 1443.
- D. Adams, A. Bénardeau, M. J. Bickerdike, J. M. Bentley, C. Bissantz, A. Bourson, I. A. Cliffe, P. Hebeisen, G. A. Kennett, A. R. Knight, C. S. Malcolm, J. Mizrahi, J.-M. Plancher, H. Richter, S. Röver, S. Taylor, S. P. Vickers, *Chimia* **2004**, *58*, 613.
- S. K. Adla, F. Sasse, G. Kelter, H.-H. Fiebig, T. Lindel, *Org. Biomol. Chem.* **2013**, *11*, 6119.
- M. Zahran, Y. Abdin, H. Salama, *Arkivoc* **2008**, *xi*, 256.
- M. A. H. Zahran, H. F. Salama, Y. G. Abdin, A. M. Gamal-Eldeen, *J. Chem. Sci.* **2010**, *122*, 587.
- M.A. -H. Zahran, T.A. -R. Salem, R. M. Samaka, H. S. Agwa, A. R. Awad, *Bioorg. Med. Chem.* **2008**, *16*, 9708.
- A. A. Guirgis, M. A. H. Zahran, A. S. Mohamed, R. M. Talaat, B. Y. Abdou, H. S. Agwa, *Int. Immunopharmacol.* **2010**, *10*, 806.
- B. Y. A. El-Aarag, T. Kasai, M. A. H. Zahran, N. I. Zakhary, T. Shigehiro, S. C. Sekhar, H. S. Agwa, A. Mizutani, H. Murakami, H. Kakuta, M. Senoln, *Int. Immunopharmacol.* **2014**, *21*, 283.
- B. El-Aarag, T. Kasai, J. Masuda, M. Zahran, H. Agwa, M. Seno, *Biomed. Pharmacother.* **2017**, *85*, 549.
- H. Wu, F. Xue, X. Xiao, Y. Qin, *J. Am. Chem. Soc.* **2010**, *132*, 14052.
- Y. Liu, S. Luo, X. Fu, F. Fang, Z. Zhuang, W. Xiong, X. Jia, H. Zhai, *Org. Lett.* **2006**, *8*, 115.
- E. Leete, *J. Org. Chem.* **1958**, *23*, 631.
- N. J. Leonard, R. C. Elderfield, *J. Org. Chem.* **1942**, *7*, 556.
- G. Saidachary, K. V. Prasad, D. Divya, A. Singh, U. Ramesh, B. Sridhar, B. C. Raju, *Eur. J. Med. Chem.* **2014**, *76*, 460.
- Y. Tsujimoto, C. M. Croce, *Proc. Natl. Acad. Sci. USA* **1986**, *83*, 5214.
- M. Balouiri, M. Sadiqi, S. K. Ibsouda, *J. Pharm. Anal.* **2016**, *6*, 71.

[44] G. Saidachary, K. V. Prasad, D. Divya, A. Singh, U. Ramesh, B. Sridhar, B. C. Raju, *Eur. J. Med. Chem.* **2014**, *76*, 460.

[45] <http://www.rcsb.org/pdb/explore.do?structureId=1kzn>.

## SUPPORTING INFORMATION

Additional Supporting Information may be found online in the supporting information tab for this article.

**How to cite this article:** Zahran MAH, El-Aarag B, Mehany ABM, Belal A, Younes AS. Design, synthesis, biological evaluations, molecular docking, and *in vivo* studies of novel phthalimide analogs. *Arch Pharm Chem Life Sci.* 2018;1-12. <https://doi.org/10.1002/ardp.201700363>